Science of the Total Environment 857 (2023) 159257

Contents lists available at ScienceDirect

Science of the Total Environment

journal homepage: www.elsevier.com/locate/scitotenv

Identification of neurotoxic compounds in cyanobacteria exudate mixtures

Yuanyan Zi [a,b,1], Justin R. Barker [b,1], Hugh J. MacIsaac [a,b], Ruihan Zhang [c], Robin Gras [d], Ying-Chih Chiang [e], Yuan Zhou [a], Fangchi Lu [e], Wenwen Cai [a,b], Chunxiao Sun [a,b], Xuexiu Chang [b,f,*]

[a] School of Ecology and Environmental Sciences, Yunnan University, Kunming 650091, PR China
[b] Great Lakes Institute for Environmental Research, University of Windsor, Windsor, ON N9 B 3P4, Canada
[c] Key Laboratory of Medicinal Chemistry for Natural Resources, Ministry of Education and Yunnan Province, School of Chemical Science and Technology, Yunnan University, Kunming 650091, China
[d] School of Computer Science, University of Windsor, ON N9B 3P4, Canada
[e] Kobilka Institute of Innovative Drug Discovery, School of Life and Health Science, The Chinese University of Hong Kong (Shenzhen), Shenzhen 518172, China
[f] College of Agronomy and Life Sciences, Kunming University, Kunming 650214, China

HIGHLIGHTS

- Activities of 354 MaE chemicals were predicted in ToxCast neurotoxicity assays.
- Neurotransmitter release, reception and reuptake were main mechanisms of action.
- We propose a potential neurotoxicity AOP for MaE.
- We identified nine neurotoxic compounds from cyanobacteria exudates.

GRAPHICAL ABSTRACT

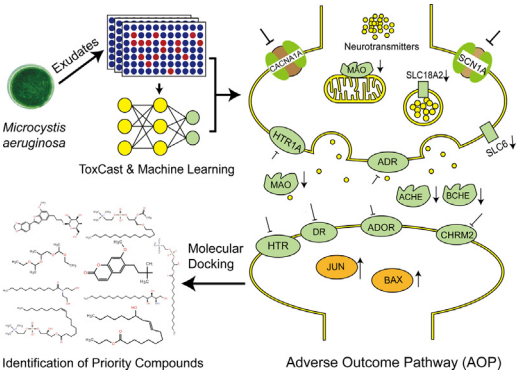

ARTICLE INFO

Editor: Shuzhen Zhang

Keywords:
Microcystis aeruginosa
Neurotoxicity
Adverse outcome pathway (AOP)
Priority substances
Machine learning

ABSTRACT

Release of toxic cyanobacterial secondary metabolites threatens biosecurity, foodwebs and public health. *Microcystis aeruginosa* (Ma), the dominant species in global freshwater cyanobacterial blooms, produces exudates (MaE) that cause adverse outcomes including nerve damage. Previously, we identified > 300 chemicals in MaE. It is critical to investigate neurotoxicity mechanisms of active substances among this suite of Ma compounds. Here, we screened 103 neurotoxicity assays from the ToxCast database to reveal targets of action of MaE using machine learning. We then built a potential Adverse Outcome Pathway (AOP) to identify neurotoxicity mechanisms of MaE as well as key targets. Finally, we selected potential neurotoxins matched with those targets using molecular docking. We found 38 targets that were inhibited and eight targets that were activated, collectively mainly related to neurotransmission (i.e. cholinergic, dopaminergic and serotonergic neurotransmitter systems). The potential AOP of MaE neurotoxicity could be caused by blocking calcium voltage-gated channel (CACNA1A), because of antagonizing neurotransmitter receptors, or because of inhibiting solute carrier transporters. We identified nine neurotoxic MaE compounds with high affinity to those targets, including LysoPC(16:0), 2-acetyl-1-alkyl-sn-glycero-3-phosphocholine, egonol glucoside, polyoxyethylene (600) monoricinoleate, and phytosphingosine. Our study enhances understanding of neurotoxicity mechanisms and identifies neurotoxins in cyanobacterial bloom exudates, which may help identify priority compounds for cyanobacteria management.

* Corresponding author at: College of Agronomy and Life Sciences, Kunming University, Kunming 650214, China.
E-mail address: xchang@uwindsor.ca (X. Chang).
[1] Equal contributions by YZ and JRB

http://dx.doi.org/10.1016/j.scitotenv.2022.159257
Received 17 August 2022; Received in revised form 1 October 2022; Accepted 1 October 2022
Available online 5 October 2022

1. Introduction

Blooming cyanobacteria pose a major risk to aquatic ecosystems and global public health (Gobler, 2020). The frequency and severity of cyanobacteria blooms (cHABs) are increasing globally and may be exacerbated by climate change (Paerl and Paul, 2012). A total of 9503 harmful algae events have been recorded worldwide as of December 2019 (Hallegraeff et al., 2021). cHABs are associated with adverse effects on other algae, plants, wild animals, livestock and humans (Lévesque et al., 2014; Buratti et al., 2017). For example, during the summer of 2018–2019, millions of fish in a river in south-eastern Australia were killed by cHABs (Ellis et al., 2022), and nearly 400 elephants in Botswana died during 2020 after drinking water containing blooming cyanobacteria (Veerman et al., 2022). Many of the 126 patients poisoned by cHABs in Caruaru, Brazil, in 1996 exhibited neurological symptoms such dizziness and vertigo (Jochimsen et al., 1998). Impacts on both wildlife and humans result from the release of a diverse mixture of potentially toxic metabolites from senescent and lysing cyanobacteria cells (Pípal et al., 2020; Banerjee et al., 2021), though toxicity of many of these metabolites remains unknown (Janssen, 2019).

Neurotoxicity is one of the most concerning hazards of cyanobacterial secondary metabolites. Some metabolites possess demonstrated neurotoxicity, including microcystins (MCs), aetokthonotoxin, anatoxin-a (ANTX-a), cylindrotoxin, and saxitoxin. MC-LR exposure caused increased brain phosphatase activity and reactive oxygen species (ROS) levels (Wang et al., 2010), decreased dopamine concentration (Wu et al., 2016), damaged the blood-brain barrier (Wang et al., 2019), and impaired cognitive and spatial learning and memory (Li et al., 2014) in a variety of species. Exposure to ANTX-a caused changes in protein expression in zebrafish brain (Carneiro et al., 2015). Cylindrotoxin increased lipid peroxidation levels and enlarged neuronal nuclei in and DNA damage to brain tissue (Guzmán-Guillén et al., 2015; Rabelo et al., 2021). Saxitoxin decreased cell viability, increased glutathione peroxidase levels, and severely damaged neuronal-cell DNA (Silva et al., 2014). Aetokthonotoxin caused vacuolar myelinopathy and associated eagle kills (Breinlinger et al., 2021). It is important to note that many cHAB toxicity studies focused on single, well-identified chemicals, though metabolites released by cyanobacteria are comprised of varying mixtures of these compounds (Bláhová et al., 2009; Janssen, 2019; Pawlik-Skowrońska et al., 2019). Thus, existing tests exploring consequences of exposure to individual chemicals, while valuable, may not be representative of the overall impact of chemical mixtures in nature (Ger et al., 2014). It is quite possible that cHAB metabolite mixtures have higher toxicity relative to single ones (Pawlik-Skowrońska et al., 2019; Hsieh et al., 2021), thus information on the combined effect of mixtures is important for ecotoxicological assessments (Qian et al., 2018). At the same time, due to the complexity of the composition of cyanobacterial metabolites, it is also important to identify priority toxins within these mixtures that are worthy of close monitoring in nature (Bláhová et al., 2009).

Microcystis aeruginosa, the most dominant bloom-forming cyanobacterium globally, produces exudates (MaE) that may exert strong inhibitory effects on co-occurring species (Jiang et al., 2019), especially if exudates were obtained from the exponential-growth phrase (Xu et al., 2016). MaE exposure is associated with adverse outcomes on aquatic biota including inhibition of growth in green algae, diatoms, and bacteria (Wang et al., 2017), estrogenic effects in zooplankton (Xu et al., 2019), and malformations in fish embryos (Zi et al., 2018). In addition, MaE can cause neurological damage and reduced fish activity (Qian et al., 2018; Cai et al., 2022). MaE also causes reduced levels of acetylcholinesterase (ACHE) and dopamine and expression of the acetylcholine receptor, affecting cholinergic and dopaminergic neurotransmitter systems (Qian et al., 2018). However, the identity of other potential neurotoxins and other mechanisms of neurotoxicity remain unknown. Thus, it is critical to increase understanding of neurotoxic chemicals in MaE as well as their effects.

We have identified 12 classes and > 300 chemicals in an MaE mixture obtained from exponential-growth cultures of *M. aeruginosa* (FACHB 905 strain) (Zhou et al., under review). The complexity of chemicals produced makes it difficult to identify major toxins and to determine mechanisms of toxicity. However, the Adverse Outcome Pathway (AOP) is a framework that assesses toxicity of chemical mixtures, allowing chemical prioritization and screening (Ankley et al., 2010; LaLone et al., 2017). AOP focuses on the cellular level and ties to adverse outcome (AO) by identifying the molecular initiating event (MIE) and linking key events (KEs) (Ankley et al., 2010), and is widely accepted by regulatory agencies (Angrish et al., 2018). The AOP framework may be particularly useful to MaE studies, as the neurotoxicity mechanisms are not well understood.

Machine learning based on the ToxCast database and molecular docking is an excellent tool by which neurotoxins can be identified in MaE and for developing an AOP. Machine learning can predict the effects of unknown metabolites after training models with known chemicals (Jones et al., 2021). It can screen large numbers of compounds in a short time and at low cost. The method is widely used in toxicity prediction, including hepatotoxicity of phytochemicals (Liu, 2018), toxicity of plastic additives (Jeong and Choi, 2020) and neurotoxicity of nanoparticles (Furxhi and Murphy, 2020). The ToxCast database provides a reliable source of training data for > 9000 environmental chemicals and 12,000 assays (Richard et al., 2016; Firman et al., 2021). After identification the intended targets of assays including ACHE, dopamine receptor (DR), cholinergic receptor muscarinic 2 (CHRM2), AOP can be built based on the information of targets (Jeong and Choi, 2020). Therefore, machine learning models and ToxCast assays can be used to recognize chemical structures correlated with active hit calls, and to predict if other chemical structures are active and thus their potential toxicity (Knight et al., 2009; Jeong et al., 2021). In this manner, we can prioritize chemicals and develop AOP, which in turn can feed into development of science-based regulatory measures (Knight et al., 2009; Ankley et al., 2010). On the other hand, when given a target protein, molecular docking can be used to screen active compounds from a ligand database (Jeong et al., 2021), and adverse outcomes and key events can be defined according to the interaction between chemicals and targets (Ankley et al., 2010; Firman et al., 2021). Consequently, these methods may be highly effective in identifying potential priority neurotoxic compounds in MaE and developing an AOP.

In this study, we addressed potential neurotoxicity mechanisms associated with MaE mixtures, developed an AOP, and identified potential neurotoxins using an in silico method. Specifically, we utilized ToxCast assays that address functioning of the nervous system, followed by machine learning (supervised gradient-boosting classifier models) based on the ToxCast assays to predict active chemicals in MaE mixtures. We then identified targets of action and proposed an AOP to reveal neurotoxicity mechanism(s) of MaE. Finally, we validated the active compounds by binding affinity with targets using molecular docking to screen priority neurotoxins.

2. Materials and methods

2.1. ToxCast assays

We used ToxCast assay summary file (Assay_Summary_190226) to select intended targets which were expressed in brain or function relevant to the nervous system and verified the corresponding function in the literature. We identified 72 intended targets (Table S1), which are mainly involved in neurotransmission and neuroinflammation. We selected 103 assays (Table S2) and collected the corresponding hit call data (chemical activity data of assays) from ToxCast database for the intended targets.

2.2. MaE source

The MaE chemical composition list was obtained from our previous study (Zhou et al., under review). In total, we identified 354 chemicals in MaE for which we were able to find structure information (Table S3). Most of the chemicals are lipids and lipid-like molecules.

2.3. Machine learning

We considered the hit call results of 103 assays from ToxCast and 8650 corresponding chemicals with active concentration at 10% of maximal activity. Not all chemicals were available for all assays. Chemical structure was represented by canonical simplified molecular-input line-entry system (SMILES) strings. In total, 8374 unique SMILES were obtained from PubChem (https://pubchem.ncbi.nlm.-nih.gov/) and 276 from ChemSpider (http://www.chemspider.com/). This process was repeated for 354 MaE chemical structures, obtained from PubChem. For molecular representation, we used RDkit (http://www.rdkit.org) to determine Morgan fingerprints with a radius of two bonds from each SMILES. Morgan fingerprints encode chemical structure as binary 2048-bit vectors through an iterative process of assigning unique identifiers to each atom to generate identifiers independent of the original atoms (Rogers and Hahn, 2010). Specifically, 0 and 1 represent the non-existence or existence, respectively, of specific circular substructures around each atom in a molecule which are predictive of biological activities (Morgan, 1965; Rogers and Hahn, 2010; Capecchi et al., 2020).

ToxCast assay datasets were unbalanced (Table S2), which potentially hindered machine learning performance. We conducted adaptive synthetic sampling (ADASYN), a resampling method for unbalanced data (Branco et al., 2016). Then we trained a supervised gradient boosting classifier to relate Morgan fingerprints to binary ToxCast activity classifications (active or inactive) for each assay. Gradient boosting classifiers are robust and adaptable with unbalanced data (Zarinabad et al., 2016). A single classifier was trained for each assay by 10-fold cross-validation after removal of MaE chemicals with known activity in training data. This cross-validation trained the model with 90% of the ToxCast data per assay, and tested the classification with the remaining 10% validation data. This process was repeated for each tenth of the data to ensure all data was trained and validated. Training data allowed the machine learning models to learn how chemical structure related to activity. Once a model was trained, validation data was used to provide a measure of model fit. Modeling and 10-fold cross-validation were conducted using Sci-kit learn toolkit in Python 3.7 (Pedregosa et al., 2011). The resulting average of the 10 runs was obtained as the training accuracy of the models (Diamantidis et al., 2000). Classifiers were optimized by comparing a range of hyperparameters and selecting the highest average accuracy and F1 values. F1 is the harmonic mean of sensitivity and precision, which is widely used to evaluate the success of binary classifiers (Lipton et al., 2014). We calculated other metrics of model performance, including true positive rate (sensitivity) and true negative rate (specificity). Final classifiers were applied to predict the activity of MaE chemicals per assay. MaE was defined as having activity in assays if the number of active compounds was > 10% (Jeong and Choi, 2020).

2.4. Molecular docking

We used Molecular Operation Environment (MOE, version 2020) (Chemical Computing Group, Ltd., Montreal, Quebec, Canada) software for molecular docking. We prepared SMILES data of predicted MaE active chemicals per assay as ligands as single text files. The ligand structure was prepared using the molecular utility's wash function. The log octanol/water partition coefficient (log K_{ow}) of active chemicals was calculated in descriptors utility of Database Viewer.

We downloaded the X-ray crystal structures of receptors from Protein Database Bank (PDB) (https://www.rcsb.org/), which matched Uniprot identifications of ToxCast assays, such as the PDB codes 7rb5 for ACHE, 5zkc for CHRM2, 7jqz for DRD1, and 2ydo for ADORA2A (adenosine A2a receptor) (Table S2). We then used the QuickPrep utility to prepare the receptors after editing them to remove water molecules (Alharbi et al., 2022).

Prepared ligands were docked into the site of receptors using Triangular Matcher placement with London dG scoring function, and further refined using rigid receptor with GBVI/WSA dG scoring function. For each ligand, 30 poses were kept and the one with the best docking score is reported. The same protocol was validated by re-docking the crystal ligands back to the protein, and good agreement between the docking poses and crystal structure was found (Table S2). Priority compounds were selected with binding affinity of lower than −6.0 Kcal/mol (Jeong et al., 2021) and molecular weight higher than 150 (Dix et al., 2006). We chose the compounds with log K_{ow} between 1.7 (Kostal et al., 2014) and 5.0 (Pajouhesh and Lenz, 2005) because of their ability to penetrate the blood-brain barrier and bind to target.

2.5. Data analysis

We calculated mean values and standard errors of model parameters. We analyzed target gene ontology (GO) biological process and molecular function using BiocManager in R v4.2.0 (Morgan, 2022). We also analyzed target Kyoto Encyclopedia of Genes and Genomes (KEGG) pathway in Cytospace v3.9.1 (Shannon et al., 2003).

3. Results

3.1. Machine learning of ToxCast assays

Across the 103 classifiers, accuracy from cross-validation ranged from 22.5 to 99.4% with an average of 82.6%. F1 values ranged from 29.4 to 99.4% with an average of 82.4% (Table S2). Depending on assay, sensitivity ranged from 31.2 to 100%, while specificity ranged from 13.3 to 100%. Owing to unbalanced data, we selected assays with F1 ≥ 70% and sensitivity ≥ 20% and specificity ≥ 20% for further steps, resulting in 86 assays with sufficient accuracy for subsequent steps (Table 1). Retained assays

Table 1
Summary of classification ability of machine learning models with F1 (≥ 70%), sensitivity (≥ 20%), and specificity (≥ 20%) by intended target families. All model performance information is provided in Table S2.

Intended target family	Number of assays	Mean model performance			
		Accuracy (SD) (%)	Sensitivity (SD) (%)	Specificity (SD) (%)	F1 (SD) (%)
GPCR	28	87.9 (0.08)	91.0 (0.09)	84.7 (0.06)	88.3 (0.08)
DNA binding	17	86.6 (0.07)	84.3 (0.08)	88.8 (0.07)	86.2 (0.08)
Transporter	7	86.4 (0.09)	90.6 (0.09)	82.2 (0.10)	87.1 (0.08)
Cell cycle	6	89.2 (0.09)	86.3 (0.10)	92.1 (0.08)	88.8 (0.09)
Ion channel	6	88.0 (0.08)	88.7 (0.07)	87.4 (0.11)	88.2 (0.08)
Oxidoreductase	5	84.8 (0.09)	88.0 (0.09)	81.8 (0.12)	85.3 (0.09)
Esterase	4	82.5 (0.05)	81.8 (0.11)	83.1 (0.06)	82.0 (0.06)
CYP	3	94.8 (0.03)	95.7 (0.03)	94.0 (0.05)	94.8 (0.03)
Kinase	3	92.4 (0.05)	89.0 (0.06)	96.0 (0.01)	91.7 (0.05)
Ligase	2	92.0 (0.03)	88.1 (0.03)	96.0 (0.01)	91.7 (0.02)
Nuclear receptor	2	92.3 (0.01)	91.2 (0.01)	93.4 (0.02)	92.2 (0.01)
Methyltransferase	1	92.5 (NA)	89.5 (NA)	95.0 (NA)	91.9 (NA)
Miscellaneous protein	1	94.5 (NA)	98.1 (NA)	91.1 (NA)	94.6 (NA)
Protease	1	78.6 (NA)	81.3 (NA)	75.8 (NA)	79.2 (NA)

SD: standard deviation; NA: not available.

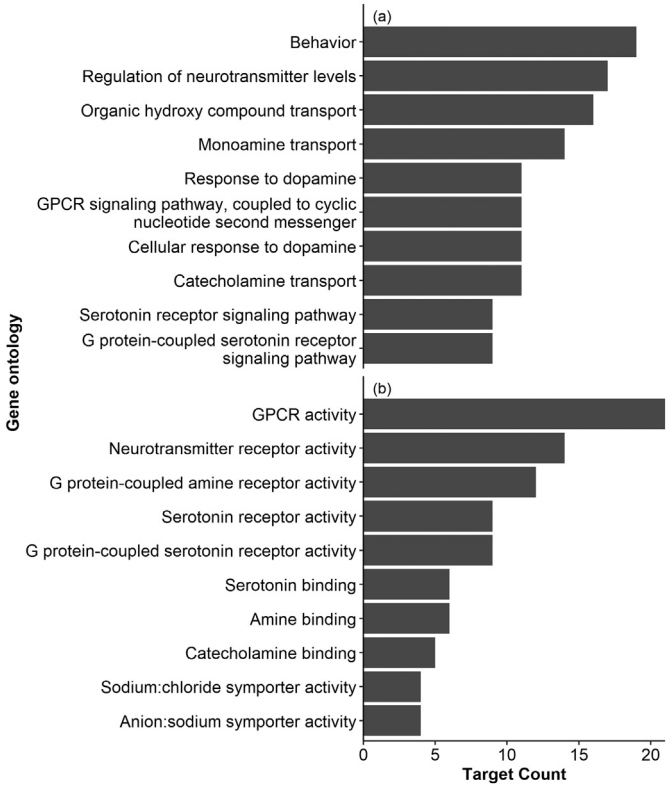

Fig. 1. Target counts of the 10 most significant GO enrichment analysis terms of biological processes (a) and molecular functions (b) domains of *Microcystis aeruginosa* exudate action targets. Target count is the number of targets in the corresponding GO term.

belonged to 17 intended target families: G protein coupled receptor (GPCR) (28 assays), DNA binding (17 assays), transporter (seven assays), cell cycle (six assays), ion channel (six assays), oxidoreductase (five assays), and other eight intended target families with fewer than five assays each.

3.2. Targets of action of MaE

We predicted activity of MaE chemicals in 86 selected assays (Table S3), of which 61 assays showed activity and could be grouped into 46 targets (Table S4). According to top 10 GO pathway enrichment analysis (Fig. 1), these 46 targets of action in the GO biological process (Fig. 1a) domain were associated with behavior, regulation of neurotransmitter levels, organic hydroxy compound transport, monoamine transport, response to dopamine, GPCR signaling pathway, cellular response to dopamine, catecholamine transport, and serotonin receptor signaling pathway terms. These targets in the GO molecular function were involved in GPCR activity (21) and includes neurotransmitter receptor activity (14), G protein-coupled amine receptor activity (12), G protein-coupled serotonin receptor activity (nine), neuropeptide receptor activity (two), and glutamate receptor activity (two). Other molecular functions were also associated with serotonin binding, amine binding, catecholamine binding, sodium: chloride symporter activity, and anion: sodium sympoter activity (Fig. 1b). Results indicated that MaE mainly affected the process of neurotransmission, such as disturbing reception and transport.

In addition, 46 targets of action were mainly involved in 15 neuro-associated KEGG pathways (Fig. 2). The neuroactive ligand-receptor interaction pathway had the most targets (21), followed by the calcium signaling pathway (12) and the serotonergic synapse (12). These targets were also involved in dopaminergic and cholinergic synapse. The pathways with the fewest targets involved were the sphingolipid signaling pathway and apoptosis and neurotrophin signaling pathway. Therefore, MaE impacted neurotransmission, particularly for serotonergic, dopaminergic, and cholinergic synapses, and were also involved in the apoptotic pathway.

Among 46 active targets, MaE had high activity in assays targeting the 5-hydroxytryptamine receptor (HTR), solute carrier (SLC), adrenoceptor (ADR), monoamine oxidase (MAO) and voltage-gated channel, while assays targeting phosphodiesterase 10A and BCL2 apoptosis regulator (BCL2) had low activity (Table S4). We found that MaE had higher activity to neurotransmission targets than to apoptosis targets. Eight targets were activated by MaE, such as Jun proto-oncogene, AP-1 transcription factor subunit (JUN), BCL2 associated X, apoptosis regulator (BAX), Sp1 transcription factor (SP1), while 38 targets were inhibited, such as calcium voltage-gated channel subunit alpha1 A (CACNA1A), sodium voltage-gated channel

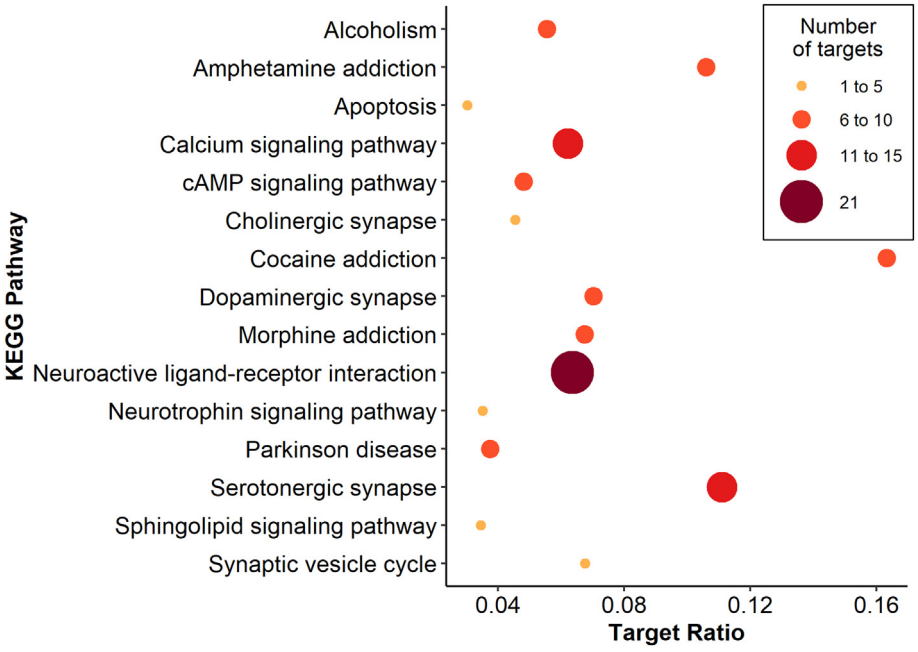

Fig. 2. Target actions of *M. aeruginosa* exudates' KEGG pathways with target ratios. Larger points indicate a higher number of targets. Target ratio details the ratio of the differential target annotated to the pathway to all proteins annotated to that pathway. The larger the target radio, the more reliable the significance of the enrichment of differential protein is in the pathway.

alpha subunit 1 (SCN1A), DRD1, ACHE, and SLC18A2. These results indicate that MaE mainly inhibited neurotransmission targets.

3.3. Potential AOP of neurotoxicity of MaE

Based on the function of targeted action (Table S2) and literature reports, we built the potential AOP of neurotoxicity of MaE, which was initiated with three MIEs (Fig. 3). MIE1 was defined as CACNA1A-blocking, which reduced synaptic vesicle release (KE1), and led to neurotransmitter imbalance (KE5) especially decreased overall neurotransmitter amounts. These events caused neurotransmission impairment (KE6) from the release process. MIE2 was defined as antagonizing neurotransmitter receptors (including presynaptic and postsynaptic receptors). Antagonism of presynaptic receptors disturbed the feedback mechanism for neurotransmitter synthesis and release (KE2), and antagonism of postsynaptic receptors blocked neural signal transportation (KE3). These two KEs then led to neurotransmitter imbalance (KE5), which in turn caused neurotransmission impairment (KE6) from the reception process. MIE3 was defined as inhibition of SLC transporters, which resulted in a reduction of neurotransmitter reuptake to presynaptic neuron (KE4). This event aggravated neurotransmitter imbalance (KE5), including causing released neurotransmitters to accumulate in the gap, which led to neurotransmission impairment (KE6) from the reuptake process. Finally, MaE caused neurotoxicity by impairing neurotransmission by inhibiting the release, reception, and uptake of neurotransmitters.

3.4. Priority compounds

Among 46 active targets screened by machine learning, 21 were obtained from PDB with X-ray structures and thence selected for molecular docking (all docking scores are provided in Table S5). From predicted MaE activity, we selected nine priority chemicals from 354 MaE chemicals based on sorting of the number of active targets, binding score, molecular weight and log K_{ow} (Table 2). All of these chemicals had binding affinity lower than −6.0 Kcal/mol, log K_{ow} between 1.9 and 4.8, and molecular weight ranging from 220 to 524. All of the priority chemicals demonstrated binding affinity for at least 14 targets. For example, LysoPC(16:0) and 2-acetyl-1-alkyl-sn-glycero-3-phosphocholine were active for 17 of 21 intended targets, respectively, 1,2-Bis(1-ethoxyethoxy)propane was active for 16 targets, egonol glucoside was active for 15 targets, and phytosphingosine was active for 14 targets.

4. Discussion

Neurotoxic compounds in MaE have received considerable attention. In this study, we identified nine priority compounds with potential for neurotoxicity. For example, among these chemicals egonol glucoside is a benzofuran which inhibits ACHE and BCHE (Liu et al., 2011). Phytosphingosine is a component of sphingolipids, the latter of which may be responsible for mediating tumor necrosis factor neurotoxicity (Martinez et al., 2012). Lysophosphatidylcholines (LysoPC) (16:0) and (18:1(9Z)) induce an increase calcium influx and stimulate inflammation response though interleukin -1β in a dose- and time-dependent manner (Liu-Wu et al., 1998; Rolin et al., 2013). 2-acetyl-1-alkyl-sn-glycero-3-phosphocholine is a pro-inflammatory mediator (Chaithra et al., 2018). We summarize that these priority compounds of MaE cause calcium dysregulation, inhibit ACHE activity, and result in inflammation and cell death. According to our AOP, these chemicals can also block CACNA1A to reduce the release of neurotransmitters, antagonize the reception of neurotransmitters to block neural signal transportation, and inhibit transporters to suppress reuptake process. These effects are consistent with the mechanism of activity of neurotoxins, such as interfering

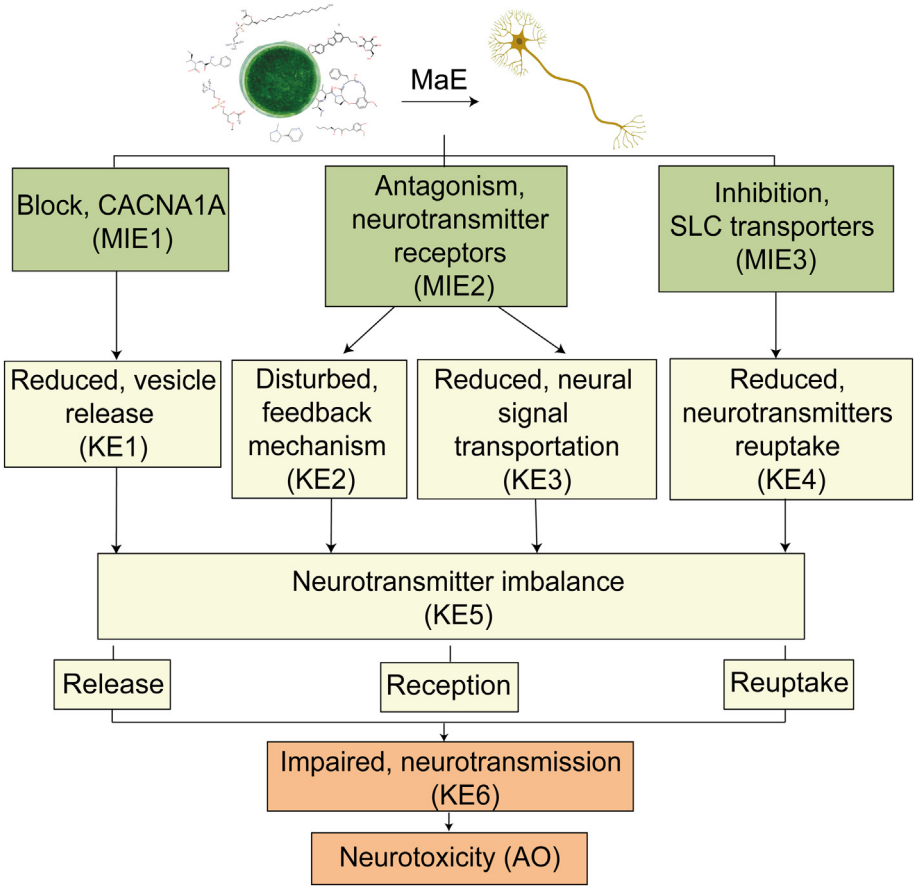

Fig. 3. The potential AOP of neurotoxicity of *M. aeruginosa* exudates (MaE).

Table 2
Potential neurotoxic compounds in MaE.

Name	Structure	Number of action targets	Log K_{ow}	Molecular weight
LysoPC(16:0)	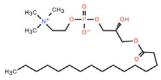	17	4.2	496.7
2-acetyl-1-alkyl-sn-glycero-3-phosphocholine	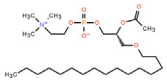	17	4.8	523.7
1,2-Bis(1-ethoxyethoxy)propane	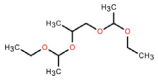	16	1.9	220.3
Egonol glucoside	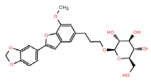	15	1.9	488.5
Lauroyl diethanolamide	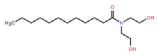	15	2.8	287.4
Polyoxyethylene (600) monoricinoleate	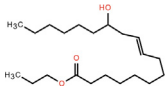	15	4.6	340.5
Dihydrosuberenol	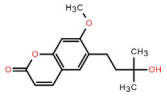	15	3.1	262.3
Phytosphingosine	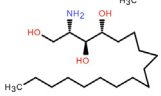	14	3.9	317.5
LysoPC(18:1(9Z))	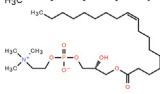	14	4.1	522.7

with neurotransmitter storage and release processes (Schiavo et al., 2000), changing ion concentrations (Parsons and du Bois, 2013), and inhibiting inter-neuron communication (Ferrari et al., 2013). Referring to KEs' relationship in AOPWiki, these effects will further result in increased cell death and decreased synaptogenesis, then cause neuroinflammation in organs, and impair learning and memory. While few of these priority compounds have been explored in neurotoxicity studies, we propose that neurotoxicity of MaE is likely related to these priority compounds. Further validation is needed for the identification of neurotoxic effects. In our other studies, we selected phytosphingosine - which has high binding affinity to our MIEs to treat human astrocyte (HA1800) – to test its neurotoxicity. We found that phytosphingosine exhibited significant neurotoxicity based on decreased nerve cell viability, abnormal nuclear morphology, elevated intracellular ROS, damaged cytoskeleton and mitochondria, and DNA damage in exposed cell cultures (unpublished data). Selected priority compounds identified herein thus warrant additional study to examine potential neurotoxic effects.

Much effort has been focused on the neurotoxicity mechanism of cyanobacterial secondary metabolites (Aráoz et al., 2010). Bioactivity evidence of priority substances and our results indicate that suppression of neurotransmission resulting from the imbalance of calcium homeostasis and the blocking of neural signals is largely responsible for the detrimental effects of MaE. This parallels that cyanobacterial neurotoxins caused harmful outcomes by acting on synapses or voltage-gated ion channels (Buratti et al., 2017). In addition, these MIEs in AOP can initiate other consequences. For example, blocking CACNA1A not only substantially hampered neurotransmission (Krick et al., 2021), but also enhanced presynaptic calcium influx (Scheuber, 2004). Reducing activity of SLC6A3 and SLC18A2 led directly to the production of hazardous alpha-Synuclein oligomers through dysregulation of dopamine levels (Bridi and Hirth, 2018) and the onset of neurodegenerative disease. Furthermore, MaE inhibited metabolic enzyme activity, blocked sodium channel (SCN1A) activity, and activated apoptotic pathways (such as JUN and BAX) (Table S4). Our recent study has validated that MaE down-regulates gene expression and content of HTR, DR, ADR and SLC in fish embryos (Cai et al., 2022), which essentially matches predicted targets of action. We systematically analyzed the target of action of MaE according to the number of active compounds, however the bioactivity of the mixture is complex and it is possible that the total effect exceeds individual effects (Hsieh et al., 2021). Therefore, the neurotoxicity of the priority compounds and their toxic contribution in MaE-induced neurotoxicity needs further attention in future studies.

Our study contributes to the identification of the neurotoxic mechanisms associated with MaE chemicals and to the screening of priority compounds for future monitoring. As problems associated with cyanobacteria are growing globally, it is crucial to identify neurotoxic substances from among the many compounds produced. There exist two main methods for monitoring the harm of cyanobacterial secondary metabolites. First, one can assess cyanobacterial cell counts in the field (e.g. Ibelings et al., 2014; Subbiah et al., 2019). This method may provide basic warnings when data on bioactivity of metabolites is lacking, but the relationship between the number of cells and the concentration of cyanotoxins is uncertain (Subbiah et al., 2019). A second, more advanced approach is to monitor for presence of specific cyanotoxins. Among the cyanobacterial toxins monitored by the United States Environmental Protection Agency, MCs are the main substances detected in *M. aeruginosa* for hepatotoxicity, while ANTX-a is monitored for nervous system damage (Loftin et al., 2016). However, only a few compounds are monitored for risk management, including ANTX-a for neurotoxins. ANTX-a is mainly produced by *Anabaena flos-aquae*. Neurotoxins and their consequences are largely ignored if cyanobacterial blooms are dominated by other species, especially with regard to *M. aeruginosa*. In this study, we screened nine priority compounds that have not been detected in the field yet. As current detection indicators are imperfect, many metabolites are not monitored with respect to potential neurotoxicity. We propose that screening of additional potential priority neurotoxins, such as phytosphingosine, be considered in future monitoring programmes.

5. Conclusion

In this study, we used machine learning supervised gradient boosting classifier models based on ToxCast assays and molecular docking to systematically

analyze potential neurotoxins present in MaE. MaE mainly inhibited neurotransmission-related targets, interfering with neurotransmitter release, reception, and reuptake mechanisms. We proposed an AOP that MaE blocked CACNA1A and antagonized neurotransmitter receptors and inhibited SLC transporters to impair neurotransmission. We screened nine priority compounds from a MaE mixture based on targets of action and suggest that these potential neurotoxins be considered in cHAB water quality monitoring programmes. This study expands our knowledge of neurotoxicity mechanism(s) and important neurotoxins of cyanobacterial blooms which will be beneficial to water security management.

CRediT authorship contribution statement

Yuanyan Zi: Methodology, Software, Formal analysis, Writing – original draft, review & editing. **Justin R. Barker:** Methodology, Software, Modeling, Writing – original draft, review & editing. **Hugh J. MacIsaac:** Conceptualization, Supervision, Funding acquisition, Writing – original draft, review & editing. **Ruihan Zhang:** Methodology, Writing – review & editing. **Robin Gras:** Methodology, Software, Modeling, Writing – review & editing. **Ying-Chih Chiang:** Methodology, Software, Writing – review & editing. **Yuan Zhou:** Resources. **Fangchi Lu:** Methodology, Software. **Wenwen Cai:** Formal analysis. **Chunxiao Sun:** Resources. **Xuexiu Chang:** Conceptualization, Supervision, Funding acquisition, Writing – review & editing.

Data availability

Data will be made available on request.

Declaration of competing interest

The authors declare that they have no known competing financial interests or personal relationships that could have appeared to influence the work reported in this paper.

Acknowledgements

This research was financially supported by National Natural Science Foundation of China (NSFC) – Yunnan Joint Key Grant (No. U1902202), Key Project of Applied Basic Research Program of Yunnan Province (No. 2019FA043), Science and Technology Innovation Team of Yunnan Provincial Department of Education (to XC), the Great Lakes Fishery Commission (2020_MAC_440940), NSERC Discovery grants (to HJM) and Canada Research Chair in Aquatic Invasive Species (to HJM).

Appendix A. Supplementary data

Supplementary data to this article can be found online at https://doi.org/10.1016/j.scitotenv.2022.159257.

References

Alharbi, A., Alsoliemy, A., Alzahrani, S.O., Alkhamis, K., Almehmadi, S.J., Khalifa, M.E., Zaky, R., El-Metwaly, N.M., 2022. Green synthesis approach for new Schiff's-base complexes; theoretical and spectral based characterization with in-vitro and in-silico screening. J. Mol. Liq. 345, 117803. https://doi.org/10.1016/j.molliq.2021.117803.

Angrish, M.M., Allard, P., McCullough, S.D., Druwe, I.L., Helbling Chadwick, L., Hines, E., Chorley, B.N., 2018. Epigenetic applications in adverse outcome pathways and environmental risk evaluation. Environ. Health Perspect. 126, 045001. https://doi.org/10.1289/ehp2322.

Ankley, G.T., Bennett, R.S., Erickson, R.J., Hoff, D.J., Hornung, M.W., Johnson, R.D., Mount, D.R., Nichols, J.W., Russom, C.L., Schmieder, P.K., Serrrano, J.A., Tietge, J.E., Villeneuve, D.L., 2010. Adverse outcome pathways: a conceptual framework to support ecotoxicology research and risk assessment. Environ. Toxicol. Chem. 29, 730–741. https://doi.org/10.1002/etc.34.

Aráoz, R., Molgó, J., Tandeau de Marsac, N., 2010. Neurotoxic cyanobacterial toxins. Toxicon 56, 813–828. https://doi.org/10.1016/j.toxicon.2009.07.036.

Banerjee, S., Maity, S., Guchhait, R., Chatterjee, A., Biswas, C., Adhikari, M., Pramanick, K., 2021. Toxic effects of cyanotoxins in teleost fish: a comprehensive review. Aquat. Toxicol. 240, 105971. https://doi.org/10.1016/j.aquatox.2021.105971.

Bláhová, L., Oravec, M., Maršálek, B., ŠEjnohová, L., Šimek, Z., Bláha, L., 2009. The first occurrence of the cyanobacterial alkaloid toxin cylindrospermopsin in the Czech Republic as determined by immunochemical and LC/MS methods. Toxicon 53, 519–524. https://doi.org/10.1016/j.toxicon.2009.01.014.

Branco, P., Torgo, L., Ribeiro, R.P., 2016. A survey of predictive modeling on imbalanced domains. ACM Comput. Surv. 49, 1–50. https://doi.org/10.1145/2907070.

Breinlinger, S., Phillips, T.J., Haram, B.N., Mareš, J., Martínez Yerena, J.A., Hrouzek, P., Sobotka, R., Henderson, W.M., Schmieder, P., Williams, S.M., Lauderdale, J.D., Wilde, H.D., Gerrin, W., Kust, A., Washington, J.W., Wagner, C., Geier, B., Liebeke, M., Enke, H., Niedermeyer, T.H.J., Wilde, S.B., 2021. Hunting the eagle killer: a cyanobacterial neurotoxin causes vacuolar myelinopathy. Science 371. https://doi.org/10.1126/science.aax9050.

Bridi, J.C., Hirth, F., 2018. Mechanisms of α-synuclein induced synaptopathy in Parkinson's disease. Front. Neurosci. 12. https://doi.org/10.3389/fnins.2018.00080.

Buratti, F.M., Manganelli, M., Vichi, S., Stefanelli, M., Scardala, S., Testai, E., Funari, E., 2017. Cyanotoxins: producing organisms, occurrence, toxicity, mechanism of action and human health toxicological risk evaluation. Arch. Toxicol. 91, 1049–1130. https://doi.org/10.1007/s00204-016-1913-6.

Cai, W., MacIsaac, H.J., Xu, R., Zhang, J., Pan, X., Zhang, Y., Yang, J., Dixon, B., Li, J., Zi, Y., Chang, X., 2022. Abnormal neurobehavior in fish early life stages after exposure to cyanobacterial exudates. Ecotoxicol. Environ. Saf. 245, 114119. https://doi.org/10.1016/j.ecoenv.2022.114119.

Capecchi, A., Probst, D., Reymond, J.L., 2020. One molecular fingerprint to rule them all: drugs, biomolecules, and the metabolome. J. Cheminf. 12. https://doi.org/10.1186/s13321-020-00445-4.

Carneiro, M., Gutiérrez-Praena, D., Osório, H., Vasconcelos, V., Carvalho, A.P., Campos, A., 2015. Proteomic analysis of anatoxin-a acute toxicity in zebrafish reveals gender specific responses and additional mechanisms of cell stress. Ecotoxicol. Environ. Saf. 120, 93–101. https://doi.org/10.1016/j.ecoenv.2015.05.031.

Chaithra, V.H., Jacob, S.P., Lakshmikanth, C.L., Sumanth, M.S., Abhilasha, K.V., Chen, C.H., Thyagarajan, A., Sahu, R.P., Travers, J.B., McIntyre, T.M., Kemparaju, K., Marathe, G.K., 2018. Modulation of inflammatory platelet-activating factor (PAF) receptor by the acyl analogue of PAF. J. Lipid Res. 59, 2063–2074. https://doi.org/10.1194/jlr.m085704.

Diamantidis, N., Karlis, D., Giakoumakis, E., 2000. Unsupervised stratification of cross-validation for accuracy estimation. Artif. Intell. 116, 1–16. https://doi.org/10.1016/s0004-3702(99)00094-6.

Dix, D.J., Houck, K.A., Martin, M.T., Richard, A.M., Setzer, R.W., Kavlock, R.J., 2006. The ToxCast program for prioritizing toxicity testing of environmental chemicals. Toxicol. Sci. 95, 5–12. https://doi.org/10.1093/toxsci/kfl103.

Ellis, I., Bates, W.B., Martin, S., McCrabb, G., Koehn, J., Heath, P., Hardman, D., 2022. How fish kills affected traditional (Baakandji) and non-traditional communities on the lower Darling-Baaka River. Mar. Freshw. Res. 73, 259. https://doi.org/10.1071/mf20376.

Ferrari, E., Gu, C., Niranjan, D., Restani, L., Rasetti-Escargueil, C., Obara, I., Geranton, S.M., Arsenault, J., Goetze, T.A., Harper, C.B., Nguyen, T.H., Maywood, E., O'Brien, J., Schiavo, G., Wheeler, D.W., Meunier, F.A., Hastings, M., Edwardson, J.M., Sesardic, D., Caleo, M., Hunt, S.P., Davletov, B., 2013. Synthetic self-assembling clostridial chimera for modulation of sensory functions. Bioconjug. Chem. 24, 1750–1759. https://doi.org/10.1021/bc4003103.

Firman, J.W., Punt, A., Cronin, M.T.D., Boobis, A.R., Wilks, M.F., Hepburn, P.A., Thiel, A., Fussell, K.C., 2021. Exploring the potential of ToxCast data in supporting read-across for evaluation of food chemical safety. Chem. Res. Toxicol. 34, 300–312. https://doi.org/10.1021/acs.chemrestox.0c00240.

Furxhi, I., Murphy, F., 2020. Predicting in vitro neurotoxicity induced by nanoparticles using machine learning. Int. J. Mol. Sci. 21, 5280. https://doi.org/10.3390/ijms21155280.

Ger, K.A., Hansson, L.A., Lürling, M., 2014. Understanding cyanobacteria-zooplankton interactions in a more eutrophic world. Freshw. Biol. 59, 1783–1798. https://doi.org/10.1111/fwb.12393.

Gobler, C.J., 2020. Climate change and harmful algal blooms: insights and perspective. Harmful Algae 91, 101731. https://doi.org/10.1016/j.hal.2019.101731.

Guzmán-Guillén, R., Manzano, I.L., Moreno, I.M., Ortega, A.I.P., Moyano, R., Blanco, A., Cameán, A.M., 2015. Cylindrospermopsin induces neurotoxicity in tilapia fish (Oreochromis niloticus) exposed to aphanizomenon ovalisporum. Aquat. Toxicol. 161, 17–24. https://doi.org/10.1016/j.aquatox.2015.01.024.

Hallegraeff, G.M., Anderson, D.M., Belin, C., Bottein, M.Y.D., Bresnan, E., Chinain, M., Enevoldsen, H., Iwataki, M., Karlson, B., McKenzie, C.H., Sunesen, I., Pitcher, G.C., Provoost, P., Richardson, A., Schweibold, L., Tester, P.A., Trainer, V.L., Yñiguez, A.T., Zingone, A., 2021. Perceived global increase in algal blooms is attributable to intensified monitoring and emerging bloom impacts. Commun. Earth Environ. 2. https://doi.org/10.1038/s43247-021-00178-8.

Hsieh, N.H., Chen, Z., Rusyn, I., Chiu, W.A., 2021. Risk characterization and probabilistic concentration–response modeling of complex environmental mixtures using new approach methodologies (NAMs) data from organotypic in vitro human stem cell assays. Environ. Health Perspect. 129, 017004. https://doi.org/10.1289/ehp7600.

Ibelings, B.W., Backer, L.C., Kardinaal, W.E.A., Chorus, I., 2014. Current approaches to cyanotoxin risk assessment and risk management around the globe. Harmful Algae 40, 63–74. https://doi.org/10.1016/j.hal.2014.10.002.

Janssen, E.M.L., 2019. Cyanobacterial peptides beyond microcystins – a review on co-occurrence, toxicity, and challenges for risk assessment. Water Res. 151, 488–499. https://doi.org/10.1016/j.watres.2018.12.048.

Jeong, J., Choi, J., 2020. Development of AOP relevant to microplastics based on toxicity mechanisms of chemical additives using ToxCastTM and deep learning models combined approach. Environ. Int. 137, 105557. https://doi.org/10.1016/j.envint.2020.105557.

Jeong, J., Bae, S.Y., Choi, J., 2021. Identification of toxicity pathway of diesel particulate matter using AOP of PPARγ inactivation leading to pulmonary fibrosis. Environ. Int. 147, 106339. https://doi.org/10.1016/j.envint.2020.106339.

Jiang, M., Zhou, Y., Wang, N., Xu, L., Zheng, Z., Zhang, J., 2019. Allelopathic effects of harmful algal extracts and exudates on biofilms on leaves of Vallisneria natans. Sci. Total Environ. 655, 823–830. https://doi.org/10.1016/j.scitotenv.2018.11.296.

Jochimsen, E.M., Carmichael, W.W., An, J., Cardo, D.M., Cookson, S.T., Holmes, C.E., Antunes, M.B., de Melo Filho, D.A., Lyra, T.M., Barreto, V.S.T., Azevedo, S.M.F.O., Jarvis, W.R., 1998. Liver failure and death after exposure to microcystins at a hemodialysis Center in Brazil. N. Engl. J. Med. 338, 873–878. https://doi.org/10.1056/nejm199803263381304.

Jones, M.R., Pinto, E., Torres, M.A., Dörr, F., Mazur-Marzec, H., Szubert, K., Tartaglione, L., Dell'Aversano, C., Miles, C.O., Beach, D.G., McCarron, P., Sivonen, K., Fewer, D.P., Jokela, J., Janssen, E.M.L., 2021. CyanoMetDB, a comprehensive public database of secondary metabolites from cyanobacteria. Water Res. 196, 117017. https://doi.org/10.1016/j.watres.2021.117017.

Knight, A.W., Little, S., Houck, K., Dix, D., Judson, R., Richard, A., McCarroll, N., Akerman, G., Yang, C., Birrell, L., Walmsley, R.M., 2009. Evaluation of high-throughput genotoxicity assays used in profiling the US EPA ToxCastTM chemicals. Regul. Toxicol. Pharmacol. 55, 188–199. https://doi.org/10.1016/j.yrtph.2009.07.004.

Kostal, J., Voutchkova-Kostal, A., Anastas, P.T., Zimmerman, J.B., 2014. Identifying and designing chemicals with minimal acute aquatic toxicity. Proc. Natl. Acad. Sci. U. S. A. 112, 6289–6294. https://doi.org/10.1073/pnas.1314991111.

Krick, N., Ryglewski, S., Pichler, A., Bikbaev, A., Götz, T., Kobler, O., Heine, M., Thomas, U., Duch, C., 2021. Separation of presynaptic Cav2 and Cav1 channel function in synaptic vesicle exo- and endocytosis by the membrane anchored Ca2+ pump PMCA. Proc. Natl. Acad. Sci. U. S. A. 118. https://doi.org/10.1073/pnas.2106621118.

LaLone, C.A., Ankley, G.T., Belanger, S.E., Embry, M.R., Hodges, G., Knapen, D., Munn, S., Perkins, E.J., Rudd, M.A., Villeneuve, D.L., Whelan, M., Willett, C., Zhang, X., Hecker, M., 2017. Advancing the adverse outcome pathway framework-an international horizon scanning approach. Environ. Toxicol. Chem. 36, 1411–1421. https://doi.org/10.1002/etc.3805.

Lévesque, B., Gervais, M.C., Chevalier, P., Gauvin, D., Anassour-Laouan-Sidi, E., Gingras, S., Fortin, N., Brisson, G., Greer, C., Bird, D., 2014. Prospective study of acute health effects in relation to exposure to cyanobacteria. Sci. Total Environ. 466–467, 397–403. https://doi.org/10.1016/j.scitotenv.2013.07.045.

Li, G., Yan, W., Cai, F., Li, C., Chen, N., Wang, J., 2014. Spatial learning and memory impairment and pathological change in rats induced by acute exposure to microcystin-LR. Environ. Toxicol. 29, 261–268. https://doi.org/10.1002/tox.21754.

Lipton, Z.C., Elkan, C., Naryanaswamy, B., 2014. Optimal thresholding of classifiers to maximize F1 measure. Machine Learning and Knowledge Discovery in Databases, pp. 225–239. https://doi.org/10.1007/978-3-662-44851-9_15.

Liu, Y., 2018. Incorporation of absorption and metabolism into liver toxicity prediction for phytochemicals: a tiered in silico QSAR approach. Food Chem. Toxicol. 118, 409–415. https://doi.org/10.1016/j.fct.2018.05.039.

Liu, J., Dumontet, V., Simonin, A.L., Iorga, B.I., Guerineau, V., Litaudon, M., Nguyen, V.H., Gueritte, F., 2011. Benzofurans from Styrax agrestis as acetylcholinesterase inhibitors: structure–activity relationships and molecular modeling studies. J. Nat. Prod. 74, 2081–2088. https://doi.org/10.1021/np200308j.

Liu-Wu, Y., Hurt-Camejo, E., Wiklund, O., 1998. Lysophosphatidylcholine induces the production of IL-1β by human monocytes. Atherosclerosis 137, 351–357. https://doi.org/10.1016/s0021-9150(97)00295-5.

Loftin, K.A., Graham, J.L., Hilborn, E.D., Lehmann, S.C., Meyer, M.T., Dietze, J.E., Griffith, C.B., 2016. Cyanotoxins in inland lakes of the United States: occurrence and potential recreational health risks in the EPA National Lakes Assessment 2007. Harmful Algae 56, 77–90. https://doi.org/10.1016/j.hal.2016.04.001.

Martinez, T.N., Chen, X., Bandyopadhyay, S., Merrill, A.H., Tansey, M.G., 2012. Ceramide sphingolipid signaling mediates tumor necrosis factor (TNF)-dependent toxicity via caspase signaling in dopaminergic neurons. Mol. Neurodegener. 7, 45. https://doi.org/10.1186/1750-1326-7-45.

Morgan, H.L., 1965. The generation of a unique machine description for chemical structures-a technique developed at chemical abstracts service. J. Chem. Doc. 5, 107–113. https://doi.org/10.1021/c160017a018.

Morgan, M., 2022. BiocManager: access the bioconductor project repository, R package version 3.30.18. https://CRAN.R-project.org/package=BiocManager.

Paerl, H.W., Paul, V.J., 2012. Climate change: links to global expansion of harmful cyanobacteria. Water Res. 46, 1349–1363. https://doi.org/10.1016/j.watres.2011.08.002.

Pajouhesh, H., Lenz, G.R., 2005. Medicinal chemical properties of successful central nervous system drugs. Neurotherapeutics 2, 541–553. https://doi.org/10.1602/neurorx.2.4.541.

Parsons, W.H., du Bois, J., 2013. Maleimide conjugates of saxitoxin as covalent inhibitors of voltage-gated sodium channels. J. Am. Chem. Soc. 135, 10582–10585. https://doi.org/10.1021/ja4019644.

Pawlik-Skowrońska, B., Toporowska, M., Mazur-Marzec, H., 2019. Effects of secondary metabolites produced by different cyanobacterial populations on the freshwater zooplankters Brachionus calyciflorus and Daphnia pulex. Environ. Sci. Pollut. Res. 26, 11793–11804. https://doi.org/10.1007/s11356-019-04543-1.

Pedregosa, F., Varoquaux, G., Gramfort, A., Michel, V., Thirion, B., Grisel, O., Blondel, M., Prettenhofer, P., Weiss, R., Dubourg, V., Vanderplas, J., Passos, A., Cournapeau, D., Brucher, M., Perrot, M., Duchesnay, E., 2011. Scikit-learn: machine learning in python. J. Mach. Learn. Res. 12, 2825–2830.

Pípal, M., Legradi, J., Smutná, M., Kočí, T., Priebojová, J., Bláhová, L., Krauss, M., Hilscherová, K., 2020. Neurobehavioral effects of cyanobacterial biomass field extracts on zebrafish embryos and potential role of retinoids. Aquat. Toxicol. 228, 105613. https://doi.org/10.1016/j.aquatox.2020.105613.

Qian, H., Liu, G., Lu, T., Sun, L., 2018. Developmental neurotoxicity of Microcystis aeruginosa in the early life stages of zebrafish. Ecotoxicol. Environ. Saf. 151, 35–41. https://doi.org/10.1016/j.ecoenv.2017.12.059.

Rabelo, J.C.S., Hanusch, A.L., Jesus, L.W.O., Mesquita, L.A., Franco, F.C., Silva, R.A., Sabóia-Morais, S.M.T., 2021. DNA damage induced by cylindrospermopsin on different tissues of the biomonitor fish Poecilia reticulata. Environ. Toxicol. 36, 1125–1134. https://doi.org/10.1002/tox.23111.

Richard, A.M., Judson, R.S., Houck, K.A., Grulke, C.M., Volarath, P., Thillainadarajah, I., Yang, C., Rathman, J., Martin, M.T., Wambaugh, J.F., Knudsen, T.B., Kancherla, J., Mansouri, K., Patlewicz, G., Williams, A.J., Little, S.B., Crofton, K.M., Thomas, R.S., 2016. ToxCast chemical landscape: paving the road to 21st century toxicology. Chem. Res. Toxicol. 29, 1225–1251. https://doi.org/10.1021/acs.chemrestox.6b00135.

Rogers, D., Hahn, M., 2010. Extended-connectivity fingerprints. J. Chem. Inf. Model. 50, 742–754. https://doi.org/10.1021/ci100050t.

Rolin, J., Al-Jaderi, Z., Maghazachi, A.A., 2013. Oxidized lipids and lysophosphatidylcholine induce the chemotaxis and intracellular calcium influx in natural killer cells. Immunobiology 218, 875–883. https://doi.org/10.1016/j.imbio.2012.10.009.

Scheuber, A., 2004. Presynaptic Cav2.1 and Cav2.2 differentially influence release dynamics at hippocampal excitatory synapses. J. Neurosci. 24, 10402–10409. https://doi.org/10.1523/jneurosci.1664-04.2004.

Schiavo, G., Matteoli, M., Montecucco, C., 2000. Neurotoxins affecting neuroexocytosis. Physiol. Rev. 80, 717–766. https://doi.org/10.1152/physrev.2000.80.2.717.

Shannon, P., Markiel, A., Ozier, O., Baliga, N.S., Wang, J.T., Ramage, D., Amin, N., Schwikowski, B., Ideker, T., 2003. Cytoscape: a software environment for integrated models of biomolecular interaction networks. Genome Res. 13, 2498–2504. https://doi.org/10.1101/gr.1239303.

Silva, C.A.D., Morais, E.C.P.D., Costa, M.D.M., Ribas, J.L.C., Guiloski, I.C., Ramsdorf, W.A., Zanata, S.M., Cestari, M.M., Oliveira Ribeiro, C.A., Magalhães, V.F., Trudeau, V.L., Silva De Assis, H.C., 2014. Saxitoxins induce cytotoxicity, genotoxicity and oxidative stress in teleost neurons in vitro. Toxicon 86, 8–15. https://doi.org/10.1016/j.toxicon.2014.04.016.

Subbiah, S., Karnjanapiboonwong, A., Maul, J.D., Wang, D., Anderson, T.A., 2019. Monitoring cyanobacterial toxins in a large reservoir: relationships with water quality parameters. PeerJ 7, e7305. https://doi.org/10.7717/peerj.7305.

Veerman, J., Kumar, A., Mishra, D.R., 2022. Exceptional landscape-wide cyanobacteria bloom in Okavango Delta, Botswana in 2020 coincided with a mass elephant die-off event. Harmful Algae 111, 102145. https://doi.org/10.1016/j.hal.2021.102145.

Wang, M., Wang, D., Lin, L., Hong, H., 2010. Protein profiles in zebrafish (Danio rerio) brains exposed to chronic microcystin-LR. Chemosphere 81, 716–724. https://doi.org/10.1016/j.chemosphere.2010.07.061.

Wang, L., Zi, J., Xu, R., Hilt, S., Hou, X., Chang, X., 2017. Allelopathic effects of Microcystis aeruginosa on green algae and a diatom: evidence from exudates addition and co-culturing. Harmful Algae 61, 56–62. https://doi.org/10.1016/j.hal.2016.11.010.

Wang, J., Zhang, C., Zhu, J., Ding, J., Chen, Y., Han, X., 2019. Blood-brain barrier disruption and inflammation reaction in mice after chronic exposure to microcystin-LR. Sci. Total Environ. 689, 662–678. https://doi.org/10.1016/j.scitotenv.2019.06.387.

Wu, Q., Yan, W., Liu, C., Li, L., Yu, L., Zhao, S., Li, G., 2016. Microcystin-LR exposure induces developmental neurotoxicity in zebrafish embryo. Environ. Pollut. 213, 793–800. https://doi.org/10.1016/j.envpol.2016.03.048.

Xu, R., Hilt, S., Pei, Y., Yin, L., Wang, X., Chang, X., 2016. Growth phase-dependent allelopathic effects of cyanobacterial exudates on Potamogeton crispus L. Seedlings. Hydrobiologia 767, 137–149. https://doi.org/10.1007/s10750-015-2489-5.

Xu, R., Jiang, Y., MacIsaac, H.J., Chen, L., Li, J., Xu, J., Wang, T., Zi, Y., Chang, X., 2019. Blooming cyanobacteria alter water flea reproduction via exudates of estrogen analogues. Sci. Total Environ. 696, 133909. https://doi.org/10.1016/j.scitotenv.2019.133909.

Zarinabad, N., Wilson, M., Gill, S.K., Manias, K.A., Davies, N.P., Peet, A.C., 2016. Multiclass imbalance learning: improving classification of pediatric brain tumors from magnetic resonance spectroscopy. Magn. Reson. Med. 77, 2114–2124. https://doi.org/10.1002/mrm.26318.

Zi, J., Pan, X., MacIsaac, H.J., Yang, J., Xu, R., Chen, S., Chang, X., 2018. Cyanobacteria blooms induce embryonic heart failure in an endangered fish species. Aquat. Toxicol. 194, 78–85. https://doi.org/10.1016/j.aquatox.2017.11.007.